

Characterization Of Leukocytes And Tissue Responses In The Bull Shark, *Carcharhinus leucas*

Deven Khanna

University of Miami, dxk405@miami.edu

Introduction

- Elasmobranchs belong to a 400 million year old clade of organisms and possess an impressive immune system with innate and adaptive defenses comparable to those found in mammals
- They also exhibit advanced wound healing and an arsenal of humoral and cellular immune defenses
- The prevailing cell types that elasmobranchs use in their immune response are the leukocytes
- There is clinical significance to the study of these leukocytes as they relate to the fields of veterinary medicine, aquaculture, and the captive care of sharks
- Understanding the relative ratio of leukocyte cell types in an organism can provide insight into an organism's health
- Assessing individual shark health, can help to make inferences about the overall population health of a species
- Leukocytes also play a crucial role in all stages of wound healing including re-epithelization, inflammation, cell proliferation with granulation, tissue formation, and tissue remodeling
- Leukocyte infiltration by neutrophils and monocytes are crucial for the inflammatory response and the signaling required to further promote growth.
- The first aim of this study was to characterize the peripheral blood leukocytes of the bull shark
- Characterizing peripheral blood leukocytes will allow researchers to establish baseline health parameters for this species and will allow this organism's health to be determined more efficiently
- The second aim was to present a case study on dermal wound healing in a bull shark caught off the coast of Miami, Florida, USA, highlighting the role of various cell types believed to be involved in the stages of wound healing

Methods

- 10 bull sharks were captured in South Florida via a circle-hook drumline system and then released once samples, sex, tag number, whole blood and size measurements were obtained
- 10 mL of whole blood gathered by caudal venipuncture was placed in 670 mOsm fixative and prepared for scanning electron microscopy, transmission electron microscopy
- Light microscopy was used to observe and count cells on peripheral blood smears prepared from whole blood in the field
- Statistical analyses were conducted using Microsoft Excel and Minitab.

Table 1. Sharks used in this study. The tag numbers, capture dates, and body size for each shark is provided. Body size was taken as total length in centimeters.

Tag number	Tag Date	Sex	Total Length (cm)
N395421	1/17/20	F	260
N395415	1/17/20	F	256
N395479	1/18/20	F	252
N395403	2/28/20	F	250
N395443	9/19/20	F	238
N395444	9/14/19	F	269
N395492	11/8/19	M	232
N395491	11/8/19	M	244
N395441	9/14/19	M	212
N395434	9/14/19	M	197

Results

Chapter I: Peripheral Blood Leukocytes

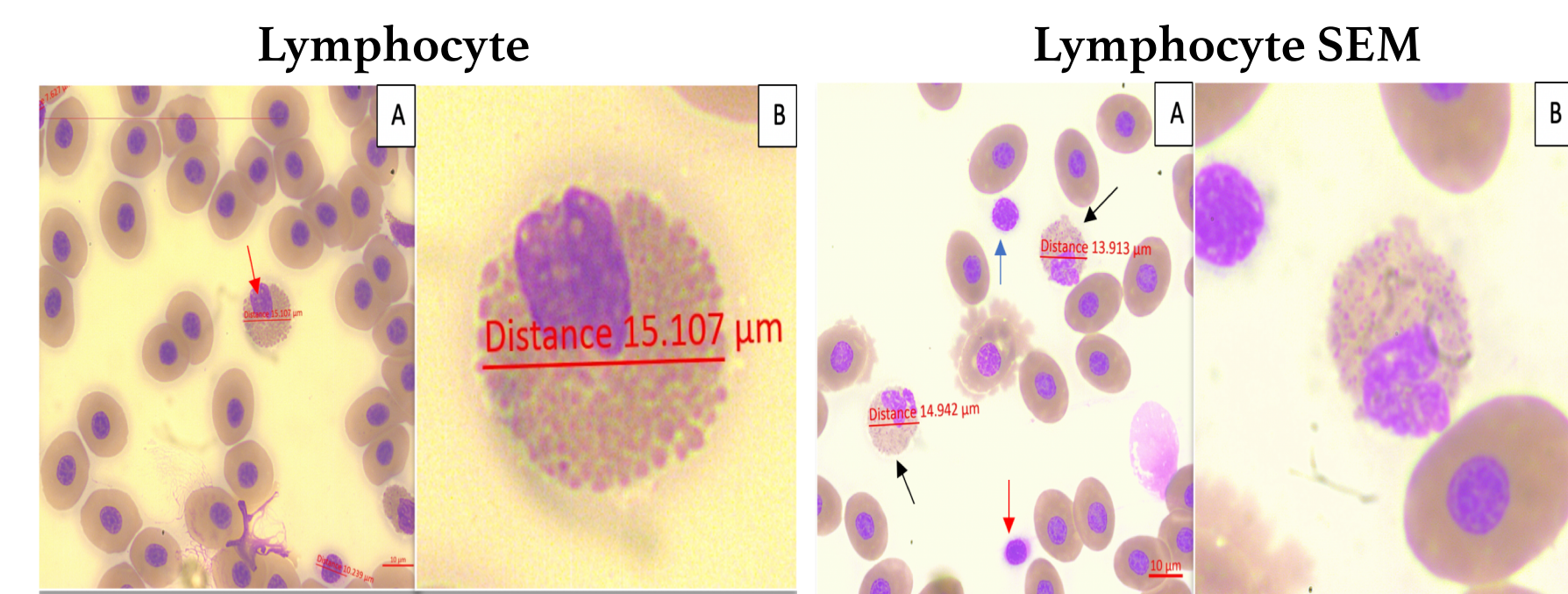
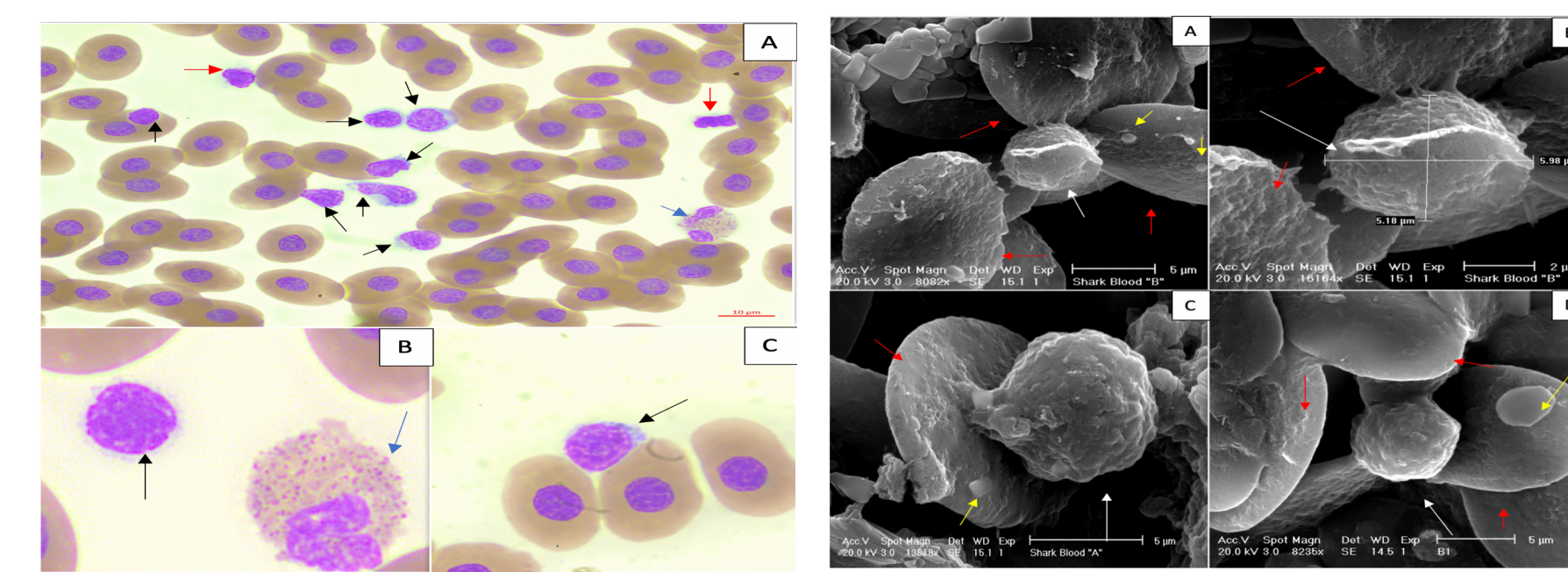


Figure 1. Lymphocytes under light microscopy. (A) 7 lymphocytes (black arrows), CEG2 Cell (blue arrow), and 2 thrombocytes (red arrows), mag: x100, scale bar: 10 (µm). (B) Large activated lymphocyte (black arrow) and CEG2 cell (blue arrow). (C) A lymphocyte (black arrow).
Figure 2. Lymphocytes under SEM. Lymphocytes (white arrows) adhered to erythrocytes with lipoproteins (yellow arrows). (A) mag: 8082x, scale bar: 5 (µm). (B) mag: 16146x, scale bar: 2 (µm). (C) mag: 13818x, scale bar: 5 (µm). (D) mag: 8235x, scale bar: 5 (µm).

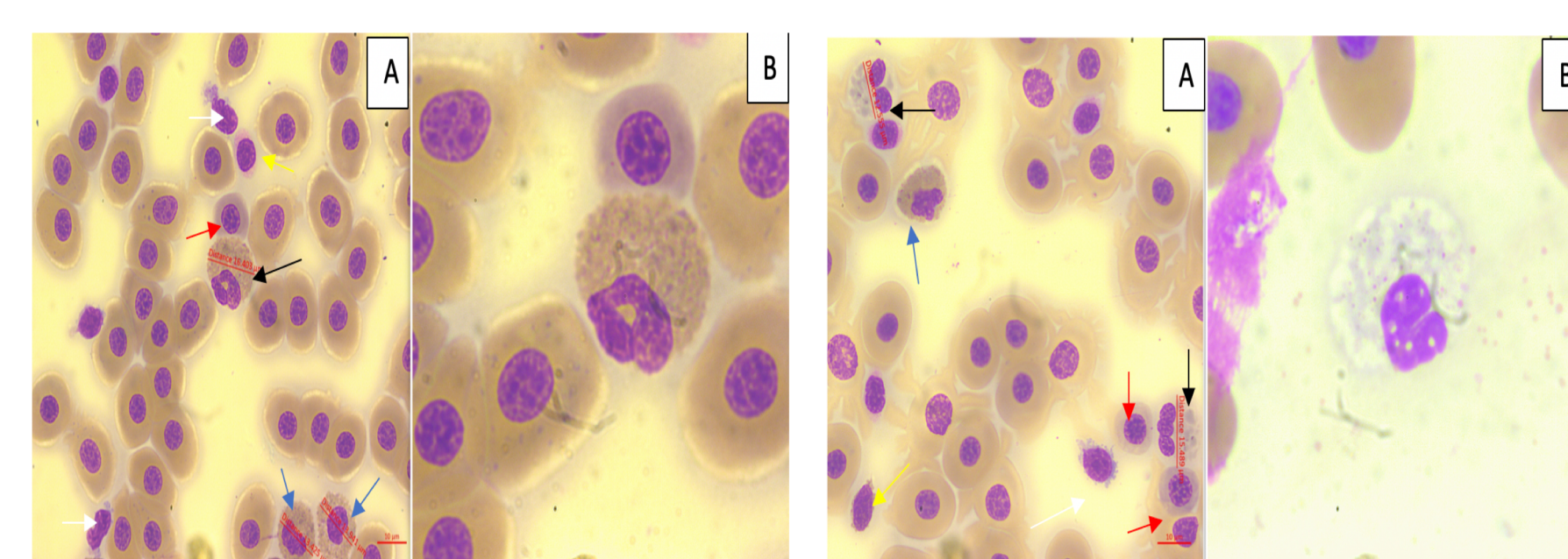


Figure 3. Course eosinophilic granulocyte under light microscopy. (A) Two CEG cells (black arrows) surrounded by erythrocytes, a thrombocyte (red arrow), and a granulated thrombocyte (yellow arrow), mag: x100, Scale bar: 10 (µm). (B) scale bar: 15,107 (µm).
Figure 4. Course eosinophilic granulocyte cell-2 (A) Two CEG cells (black arrows) surrounded by erythrocytes, thrombocyte (red arrow), activated large lymphocyte (yellow arrow), and an FEG (white arrow), mag: x100, scale bar: 10 (µm). (B) Dark course granulation present in CEG2.

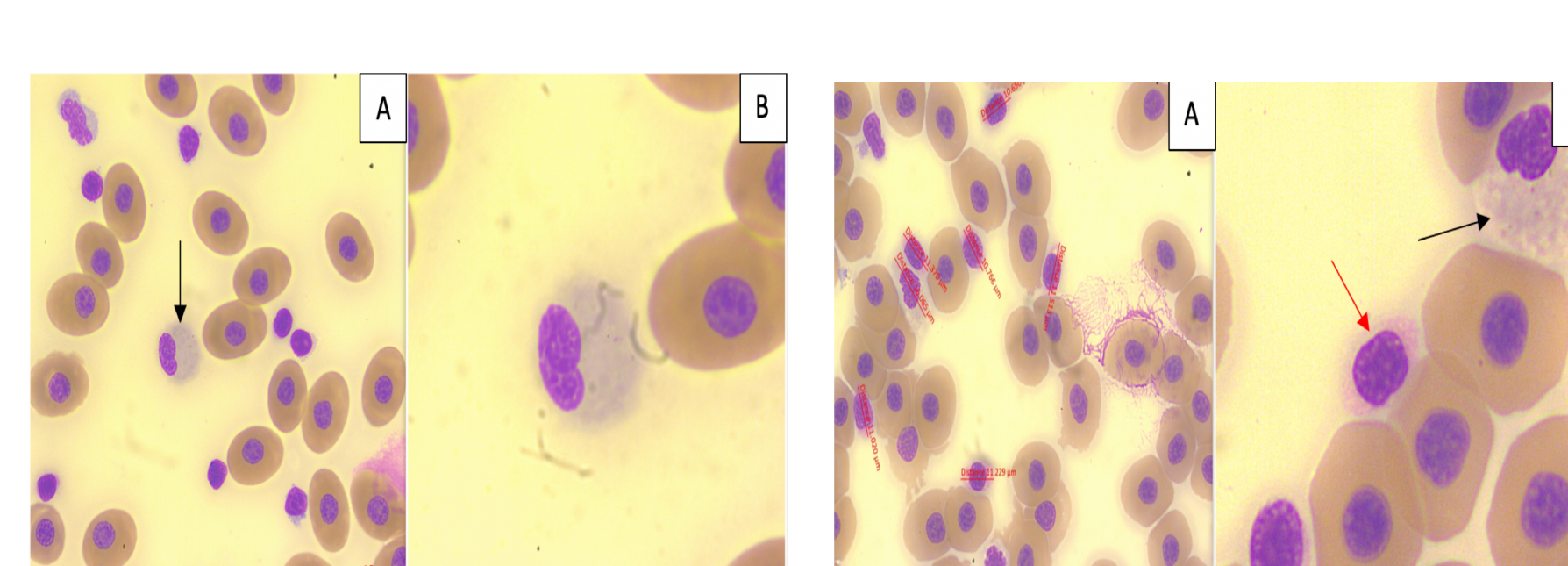


Figure 5. Fine eosinophilic granulocyte (A) FEG cell (black arrow) measured: 16,403 (µm), erythroblast (red arrow), Thrombocyte (yellow arrow), lymphocytes (white arrows), and CEG2 (blue arrow), mag: x100, scale bar: 10 (µm). (B) Fine granulation in FEG cytoplasm.

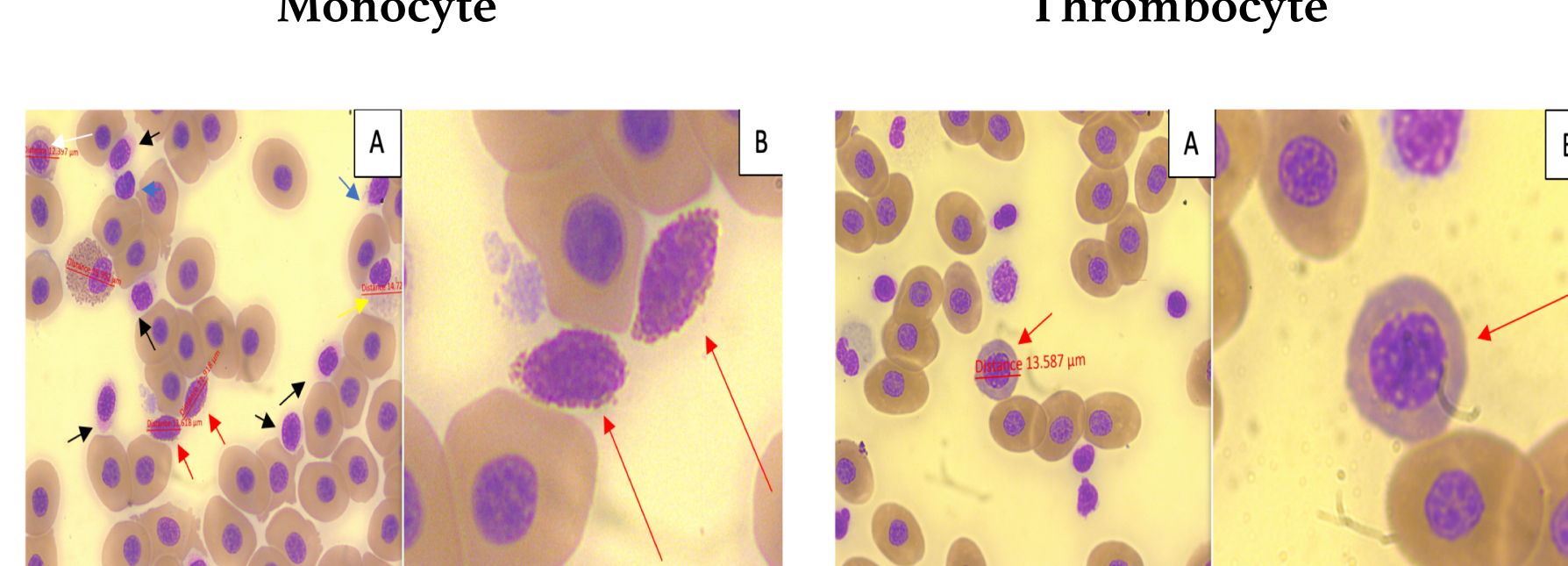


Figure 6. Neutrophil under light microscopy. (A) Trilobed basophilic nucleus (black arrows), Granulated Thrombocyte (yellow arrow), lymphocytes (white arrows), CEG2 (blue arrow), thrombocyte (orange arrow), erythroblast (red arrows), mag: x100, scale bar: 10 (µm). (B) Neutrophil with pink granulation.

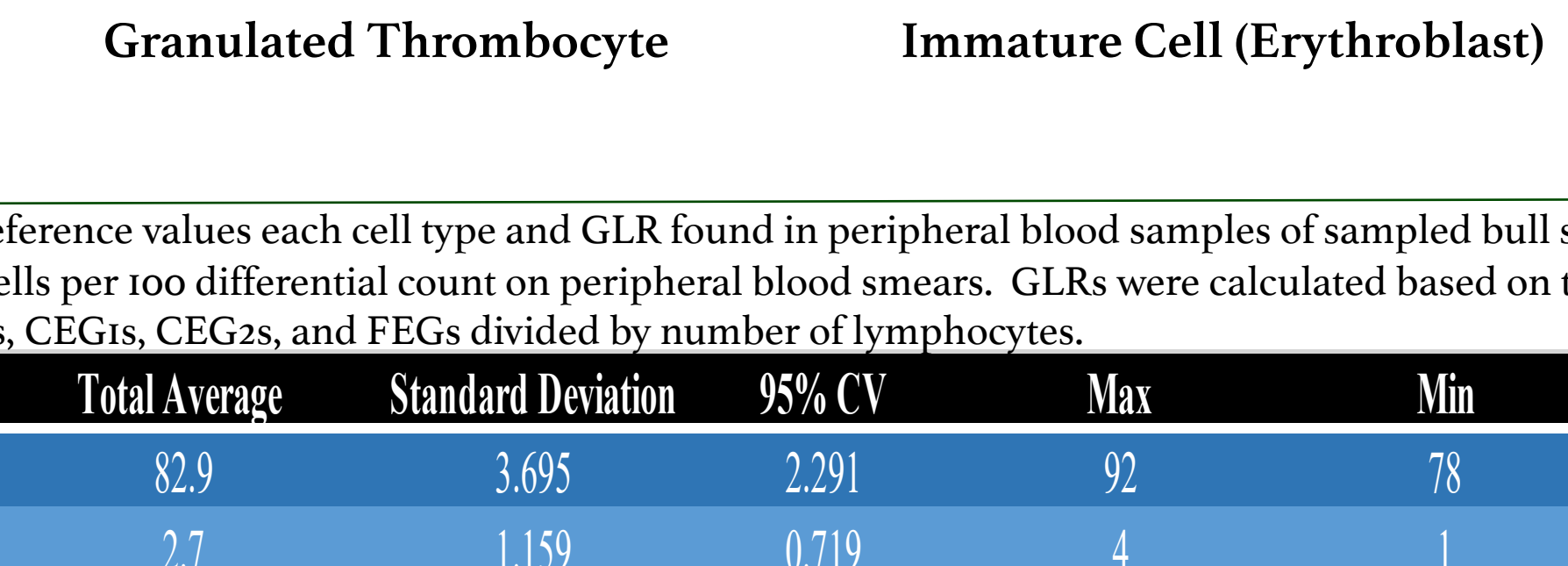


Figure 7. Monocyte under light microscopy. (A) Agranular monocyte cell mag: x100, scale bar: 10 (µm). (B) Translucent cytoplasm of agranular monocyte.

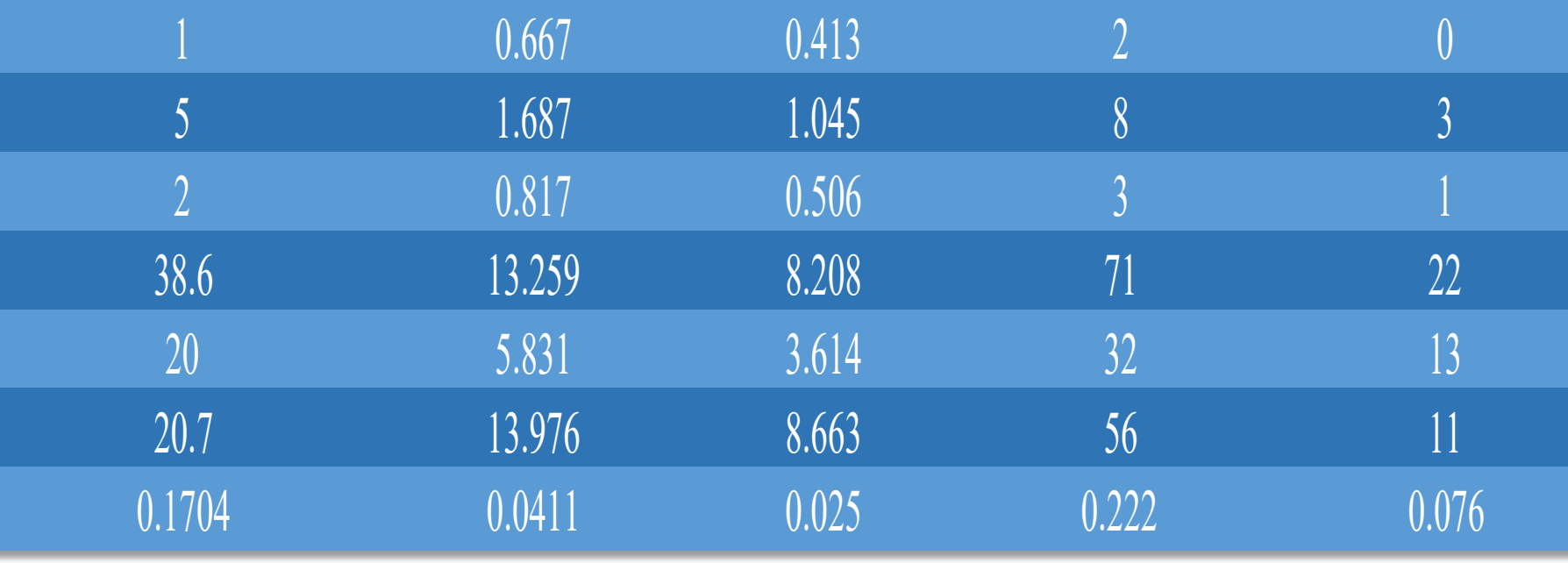


Figure 8. The thrombocyte under light microscopy. (A) Eight Thrombocyte cells (measured) mag: x100, scale bar: 10 (µm). (B) Thrombocytes with pink cytoplasm (red arrows) and neutrophil (black arrow).

Figure 9. The granulated thrombocyte under light microscopy. (A) Two granulated thrombocyte cells (red arrows), an erythroblast (white arrow), five thrombocytes (black arrows), a neutrophil (yellow arrow), and two lymphocytes (blue arrow), mag: x100, scale bar: 10 (µm). (B) Thrombocytes present pink stained granules surrounding the basophilic nucleus (red arrows).
Figure 10. Erythroblast under light microscopy. (A) The light micrograph shows the light purple cytoplasm and basophilic nucleus of the erythroblast (red arrows), mag: 100x, scale bar: 10 (µm). (B) Erythroblast, diameter: 13,587 (µm).

Figure 9. The granulated thrombocyte under light microscopy. (A) Two granulated thrombocyte cells (red arrows), an erythroblast (white arrow), five thrombocytes (black arrows), a neutrophil (yellow arrow), and two lymphocytes (blue arrow), mag: x100, scale bar: 10 (µm). (B) Thrombocytes present pink stained granules surrounding the basophilic nucleus (red arrows).

Figure 10. Erythroblast under light microscopy. (A) The light micrograph shows the light purple cytoplasm and basophilic nucleus of the erythroblast (red arrows), mag: 100x, scale bar: 10 (µm). (B) Erythroblast, diameter: 13,587 (µm).

Figure 11. Bull Shark Wound. Figure 12. Organization of cells in pink region biopsy (A) Increased re-epithelization by fibroblast action, mag: 3563x, scale bar: 20 (µm). (B) SEM of collagen fibril network in later stage of wound healing, mag: 14251x, scale bar: 5 (µm). (C) Organized fibroblasts and fibroblast expressing pseudopodia (red arrow), mag: 2300, scale bar: 20 (µm). (D) Monocyte in wound (red arrow), while infiltration of fibroblasts occurs, (yellow arrow), mag: 8000x, scale bar: 5 (µm).
Figure 13. Cellular disorganization of early stage of healing response. Collagen synthesis acting as preliminary barrier to external environment (A) Mag: 499x, scale bar: 100 (µm). (B) Mag: 1637x, scale bar: 20 (µm). (C) Mag: 3688x, scale bar: 20 (µm). (D) Mag: 6547x, scale bar: 10 (µm).
Figure 14. Cellular disorganization and initial re-epithelization seen under both SEM and TEM in various stages.
Figure 15. Cellular disorganization under TEM. (A) Mag: 2500x, scale bar: 20 (µm). (B) Mag: 2500x, scale bar: 20 (µm). (C) Initial fibroblast presence, mag: 1500x, scale bar: 20 (µm). (D) Presence of plasma-like cell (red arrow) and pseudopodia lymphoid-like cell, mag: 10000x, scale bar: 5 (µm).

Figure 11. Bull Shark Wound. Figure 12. Organization of cells in pink region biopsy (A) Increased re-epithelization by fibroblast action, mag: 3563x, scale bar: 20 (µm). (B) SEM of collagen fibril network in later stage of wound healing, mag: 14251x, scale bar: 5 (µm). (C) Organized fibroblasts and fibroblast expressing pseudopodia (red arrow), mag: 2300, scale bar: 20 (µm). (D) Monocyte in wound (red arrow), while infiltration of fibroblasts occurs, (yellow arrow), mag: 8000x, scale bar: 5 (µm).
Figure 13. Cellular disorganization of early stage of healing response. Collagen synthesis acting as preliminary barrier to external environment (A) Mag: 499x, scale bar: 100 (µm). (B) Mag: 1637x, scale bar: 20 (µm). (C) Mag: 3688x, scale bar: 20 (µm). (D) Mag: 6547x, scale bar: 10 (µm).
Figure 14. Cellular disorganization and initial re-epithelization seen under both SEM and TEM in various stages.
Figure 15. Cellular disorganization under TEM. (A) Mag: 2500x, scale bar: 20 (µm). (B) Mag: 2500x, scale bar: 20 (µm). (C) Initial fibroblast presence, mag: 1500x, scale bar: 20 (µm). (D) Presence of plasma-like cell (red arrow) and pseudopodia lymphoid-like cell, mag: 10000x, scale bar: 5 (µm).

Figure 16. Erythrocytes intertwined in fibrous material in wound of bull shark SEM. (A) Mag: 6861x, scale bar: 10 (µm). (B) Mag: 6855x, scale bar: 10 (µm).
Figure 17. Leukocytes and collagen fibrils under TEM. (A) Monocyte (red arrow), with infiltration of fibroblasts, (yellow arrow), mag: 8000x, scale bar: 5 (µm). (B) Possible lymphoid lineage cell, mag: 10000x, scale bar: 5 (µm). (C) Lymphocyte, mag: 15000, scale bar: 2 (µm). (D) Lymphocyte-like cell expressing pseudopodia, mag: 25000x, scale bar: 2 (µm).
Figure 18. Plasma-like cells under TEM. (A) Plasma-like cell (red arrow) with high degree of ER dilation, mag: 6000x, scale bar: 10 (µm). (B-D) Morphology of plasma-like cell with differences in nucleus shape, mag: 15000, scale bar: 2 (µm).
Figure 19. Fibroblast-like cells with high concentration of mitochondria under TEM. (A) Fibroblast-like cell surrounded cellular debris, mag: 8000x, scale bar: 5 (µm). (B-D) Fibroblast-like cells, mag: 8000x, scale bar: 5 (µm).
Figure 20. Virus-like presence in wounded integument under TEM. (A) Viral-like presence near cross-sectional collagen fibril formation acting as a barrier to the external environment, mag: 8000x, scale bar: 5 (µm). Inset size: 400nm. (B) Virus like vacuoles (red arrows), mag: 80000x, scale bar: 500 nm.
Figure 21. Unknown cell types observed in wound under TEM.

Figure 16. Erythrocytes intertwined in fibrous material in wound of bull shark SEM. (A) Mag: 6861x, scale bar: 10 (µm). (B) Mag: 6855x, scale bar: 10 (µm).
Figure 17. Leukocytes and collagen fibrils under TEM. (A) Monocyte (red arrow), with infiltration of fibroblasts, (yellow arrow), mag: 8000x, scale bar: 5 (µm). (B) Possible lymphoid lineage cell, mag: 10000x, scale bar: 5 (µm). (C) Lymphocyte, mag: 15000, scale bar: 2 (µm). (D) Lymphocyte-like cell expressing pseudopodia, mag: 25000x, scale bar: 2 (µm).
Figure 18. Plasma-like cells under TEM. (A) Plasma-like cell (red arrow) with high degree of ER dilation, mag: 6000x, scale bar: 10 (µm). (B-D) Morphology of plasma-like cell with differences in nucleus shape, mag: 15000, scale bar: 2 (µm).
Figure 19. Fibroblast-like cells with high concentration of mitochondria under TEM. (A) Fibroblast-like cell surrounded cellular debris, mag: 8000x, scale bar: 5 (µm). (B-D) Fibroblast-like cells, mag: 8000x, scale bar: 5 (µm).
Figure 20. Virus-like presence in wounded integument under TEM. (A) Viral-like presence near cross-sectional collagen fibril formation acting as a barrier to the external environment, mag: 8000x, scale bar: 5 (µm). Inset size: 400nm. (B) Virus like vacuoles (red arrows), mag: 80000x, scale bar: 500 nm.
Figure 21. Unknown cell types observed in wound under TEM.

Figure 19. Fibroblast-like cells with high concentration of mitochondria under TEM. (A) Fibroblast-like cell surrounded cellular debris, mag: 8000x, scale bar: 5 (µm). (B-D) Fibroblast-like cells, mag: 8000x, scale bar: 5 (µm).
Figure 20. Virus-like presence in wounded integument under TEM. (A) Viral-like presence near cross-sectional collagen fibril formation acting as a barrier to the external environment, mag: 8000x, scale bar: 5 (µm). Inset size: 400nm. (B) Virus like vacuoles (red arrows), mag: 80000x, scale bar: 500 nm.
Figure 21. Unknown cell types observed in wound under TEM.

Figure 20. Virus-like presence in wounded integument under TEM. (A) Viral-like presence near cross-sectional collagen fibril formation acting as a barrier to the external environment, mag: 8000x, scale bar: 5 (µm). Inset size: 400nm. (B) Virus like vacuoles (red arrows), mag: 80000x, scale bar: 500 nm.
Figure 21. Unknown cell types observed in wound under TEM.

Figure 21. Unknown cell types observed in wound under TEM.

Table 2. Reference values each cell type and GLR found in peripheral blood samples of sampled bull sharks. Numbers are mean cells per 100 differential count on peripheral blood smears. GLRs were calculated based on total number of neutrophils, CEGs, CEG2s, and FEGs divided by number of lymphocytes.

Cell Type	Total Average	Standard Deviation	95% CV	Max	Min	Median
Lymphocyte	82.9	3.695	2.291	92	78	82.5
CEG	2.7	1.159	0.719	4	1	3
CEG2	5.2	1.687	1.045	8	2	5
FEG	1	0.667	0.413	2	0	5.5
Neutrophil	5	1.687	1.045	8	3	5.5
Monocyte	2	0.817	0.506	3	1	2
Thrombocyte	38.6	13.259	8.208	71	22	36
GT	20	5.831	3.614	32	13	18.5
Erythroblast	20.7	13.976	8.663	56	11	14
GLR	0.1704	0.0411	0.025	0.222	0.076	0.181

Table 3. Cell diameters of various peripheral blood leukocytes in bull sharks. Mean, Max, Min, and Median of cell sizes are given in micrometers using Zenn software program under 100x light microscopy.

Cell Type	Average Diameter (µm)	Standard Deviation	95% CV	Max Diameter (µm)	Min Diameter (µm)	Median (µm)
Lymphocyte	8.64	2.029	1.258	13.69	6.78	8.35
CEG	14.45	0.832	0.515	15.58	13.35	14.34
CEG2	11.08	0.502	0.311	11.81	10.31	11.13
FEG	15.11	0.951	0.589	16.41	13.43	15.35
Neutrophil	15.74	1.225	0.759	17.71	14.33	15.41
Monocyte	11.01	1.230	0.762	13.62	9.12	10.91
Thrombocyte	10.87	0.515	0.319	11.51	9.87	10.91
GT	13.28	1.761	1.092	15.86	11.12	12.81
Erythroblast	12.59	1.450	0.899	14.07	8.36	12.31
Erythrocyte	12.58	1.111	0.689	14.07	11.08	12.67

Chapter II: Tissue Response to Wounding



Figure 11. Bull Shark Wound. Figure 12. Organization of cells in pink region biopsy (A) Increased re-epithelization by fibroblast action, mag: 3563x, scale bar: 20 (µm). (B) SEM of collagen fibril network in later stage of wound healing, mag: 14251x, scale bar: 5 (µm). (C) Organized fibroblasts and fibroblast expressing pseudopodia (red arrow), mag: 2300, scale bar: 20 (µm). (D) Monocyte in wound (red arrow), while infiltration of fibroblasts occurs, (yellow arrow), mag: 8000x, scale bar: 5 (µm).
Figure 13. Cellular disorganization of early stage of healing response. Collagen synthesis acting as preliminary barrier to external environment (A) Mag: 499x, scale bar: 100 (µm). (B) Mag: 1637x, scale bar: 20 (µm). (C) Mag: 3688x, scale bar: 20 (µm). (D) Mag: 6547x, scale bar: 10 (µm).
Figure 14. Cellular disorganization and initial re-epithelization seen under both SEM and TEM in various stages.
Figure 15. Cellular disorganization under TEM. (A) Mag: 2500x, scale bar: 20 (µm). (B) Mag: 2500x, scale bar: 20 (µm). (C) Initial fibroblast presence, mag: 1500x, scale bar: 20 (µm). (D) Presence of plasma-like cell (red arrow) and pseudopodia lymphoid-like cell, mag: 10000x, scale bar: 5 (µm).

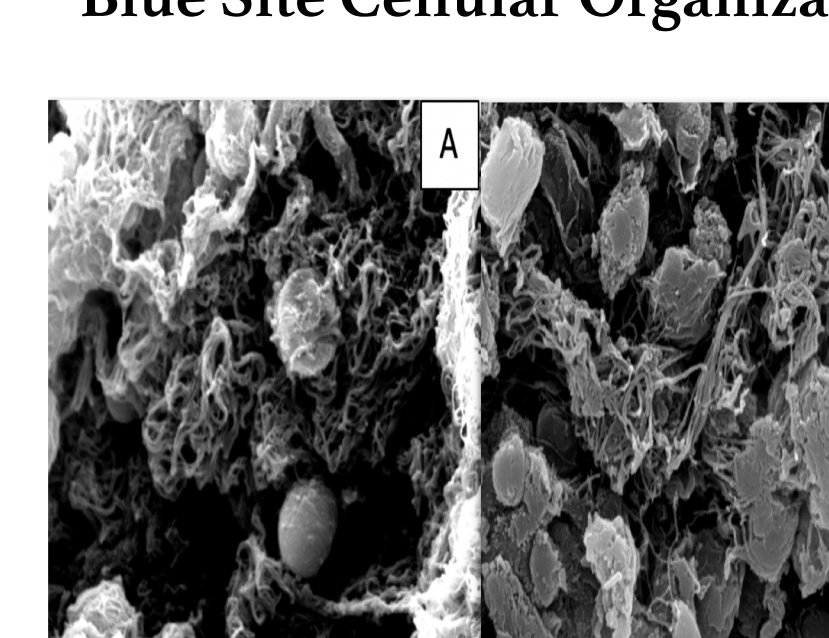


Figure 16. Erythrocytes intertwined in fibrous material in wound of bull shark SEM. (A) Mag: 6861x, scale bar: 10 (µm). (B) Mag: 6855x, scale bar: 10 (µm).
Figure 17. Leukocytes and collagen fibrils under TEM. (A) Monocyte (red arrow), with infiltration of fibroblasts, (yellow arrow), mag: 8000x, scale bar: 5 (µm). (B) Possible lymphoid lineage cell, mag: 10000x, scale bar: 5 (µm). (C) Lymphocyte, mag: 15000, scale bar: 2 (µm). (D) Lymphocyte-like cell expressing pseudopodia, mag: 25000x, scale bar: 2 (µm).
Figure 18. Plasma-like cells under TEM. (A) Plasma-like cell (red arrow) with high degree of ER dilation, mag: 6000x, scale bar: 10 (µm). (B-D) Morphology of plasma-like cell with differences in nucleus shape, mag: 15000, scale bar: 2 (µm).
Figure 19. Fibroblast-like cells with high concentration of mitochondria under TEM. (A) Fibroblast-like cell surrounded cellular debris, mag: 8000x, scale bar: 5 (µm). (B-D) Fibroblast-like cells, mag: 8000x, scale bar: 5 (µm).
Figure 20. Virus-like presence in wounded integument under TEM. (A) Viral-like presence near cross-sectional collagen fibril formation acting as a barrier to the external environment, mag: 8000x, scale bar: 5 (µm). Inset size: 400nm. (B) Virus like vacuoles (red arrows), mag: 80000x, scale bar: 500 nm.
Figure 21. Unknown cell types observed in wound under TEM.

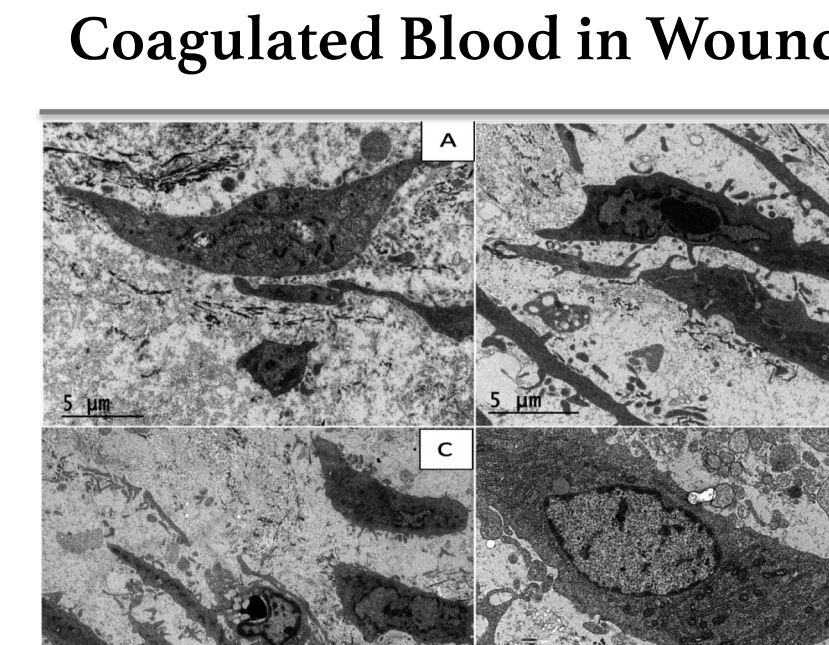


Figure 17. Leukocytes and collagen fibrils under TEM. (A) Monocyte (red arrow), with infiltration of fibroblasts, (yellow arrow), mag: 8000x, scale bar: 5 (µm). (B) Possible lymphoid lineage cell, mag: 10000x, scale bar: 5 (µm). (C) Lymphocyte, mag: 15000, scale bar: 2 (µm). (D) Lymphocyte-like cell expressing pseudopodia, mag: 25000x, scale bar: 2 (µm).
Figure 18. Plasma-like cells under TEM. (A) Plasma-like cell (red arrow) with high degree of ER dilation, mag: 6000x, scale bar: 10 (µm). (B-D) Morphology of plasma-like cell with differences in nucleus shape, mag: 15000, scale bar: 2 (µm).
Figure 19. Fibroblast-like cells with high concentration of mitochondria under TEM. (A) Fibroblast-like cell surrounded cellular debris, mag: 8000x, scale bar: 5 (µm). (B-D) Fibroblast-like cells, mag: 8000x, scale bar: 5 (µm).
Figure 20. Virus-like presence in wounded integument under TEM. (A) Viral-like presence near cross-sectional collagen fibril formation acting as a barrier to the external environment, mag: 8000x, scale bar: 5 (µm). Inset size: 400nm. (B) Virus like vacuoles (red arrows), mag: 80000x, scale bar: 500 nm.
Figure 21. Unknown cell types observed in wound under TEM.

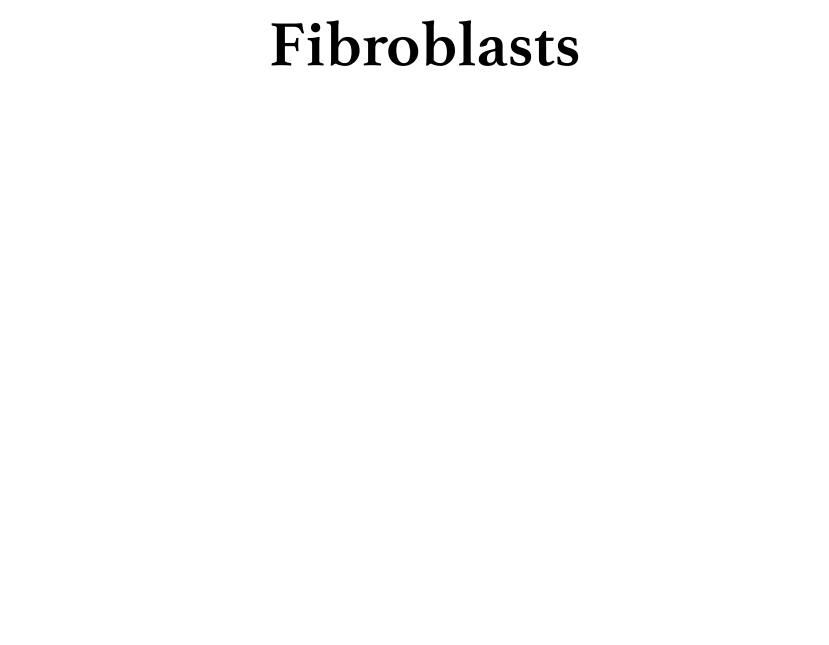


Figure 18. Plasma-like cells under TEM. (A) Plasma-like cell (red arrow) with high degree of ER dilation, mag: 6000x, scale bar: 10 (µm). (B-D) Morphology of plasma-like cell with differences in nucleus shape, mag: 15000, scale bar: 2 (µm).
Figure 19. Fibroblast-like cells with high concentration of mitochondria under TEM. (A) Fibroblast-like cell surrounded cellular debris, mag: 8000x, scale bar: 5 (µm). (B-D) Fibroblast-like cells, mag: 8000x, scale bar: 5 (µm).
Figure 20. Virus-like presence in wounded integument under TEM. (A) Viral-like presence near cross-sectional collagen fibril formation acting as a barrier to the external environment, mag: 8000x, scale bar: 5 (µm). Inset size: 400nm. (B) Virus like vacuoles (red arrows), mag: 80000x, scale bar: 500 nm.
Figure 21. Unknown cell types observed in wound under TEM.

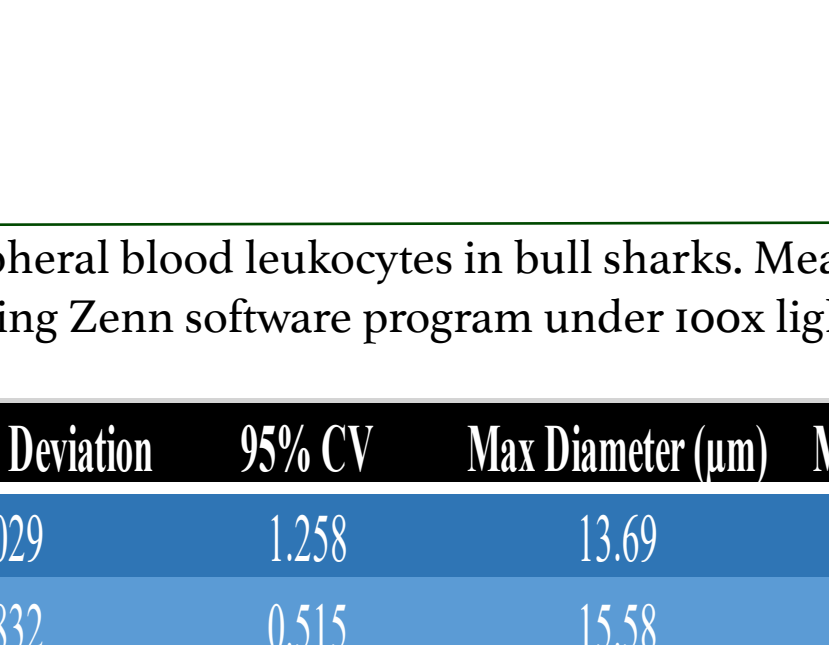


Figure 19. Fibroblast-like cells with high concentration of mitochondria under TEM. (A) Fibroblast-like cell surrounded cellular debris, mag: 8000x, scale bar: 5 (µm). (B-D) Fibroblast-like cells, mag: 8000x, scale bar: 5 (µm).
Figure 20. Virus-like presence in wounded integument under TEM. (A) Viral-like presence near cross-sectional collagen fibril formation acting as a barrier to the external environment, mag: 8000x, scale bar: 5 (µm). Inset size: 400nm. (B) Virus like vacuoles (red arrows), mag: 80000x, scale bar: 500 nm.
Figure 21. Unknown cell types observed in wound under TEM.

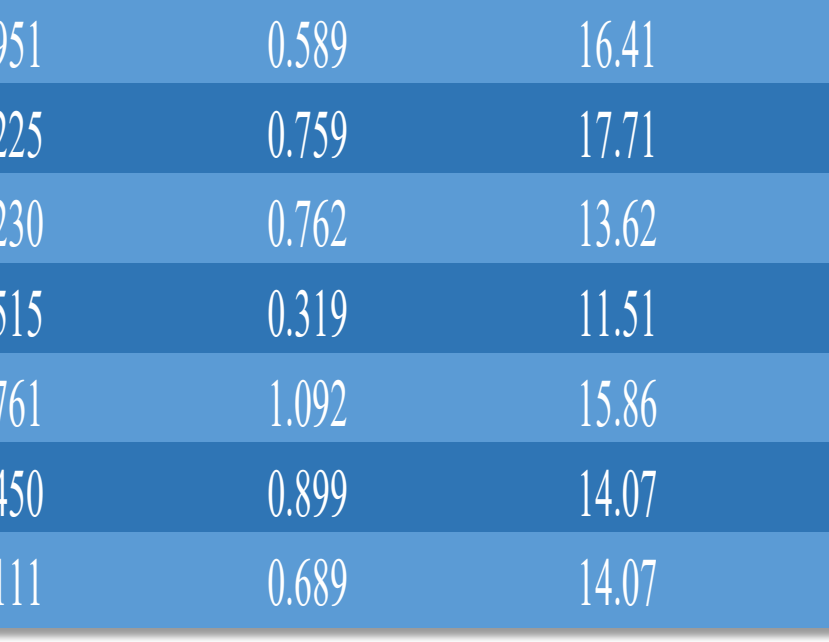


Figure 20. Virus-like presence in wounded integument under TEM. (A) Viral-like presence near cross-sectional collagen fibril formation acting as a barrier to the external environment, mag: 8000x, scale bar: 5 (µm). Inset size: 400nm. (B) Virus like vacuoles (red arrows), mag: 80000x, scale bar: 500 nm.
Figure 21. Unknown cell types observed in wound under TEM.

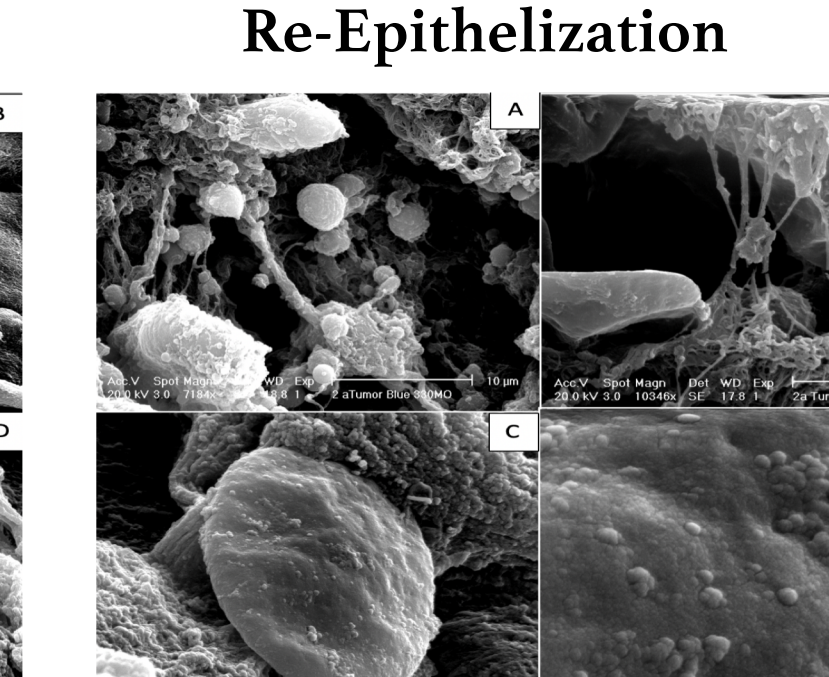
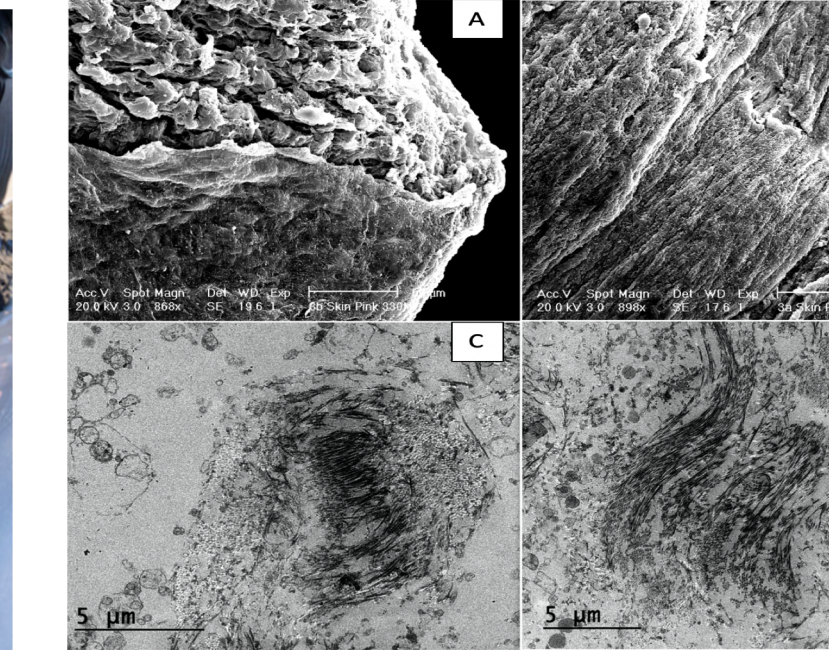


Figure 21. Unknown cell types observed in wound under TEM.

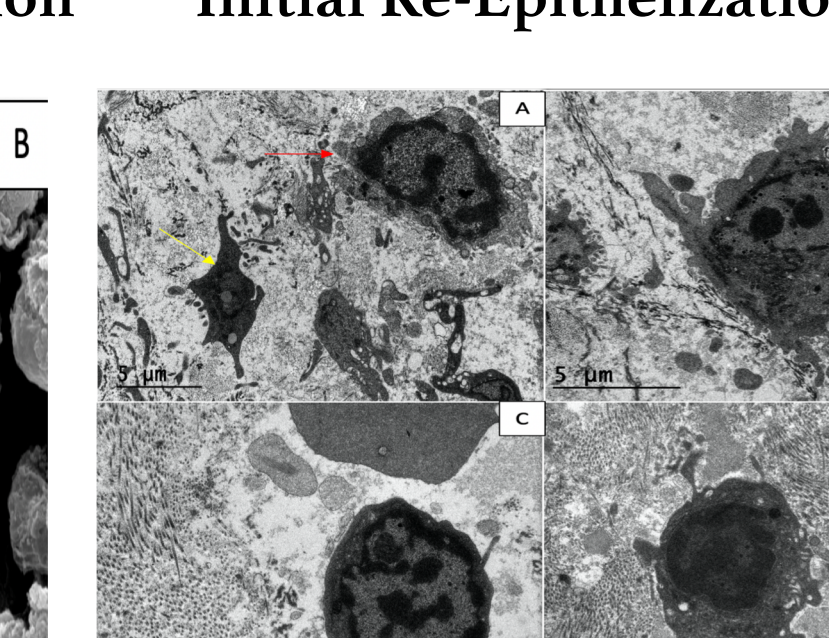


Figure 21. Unknown cell types observed in wound under TEM.

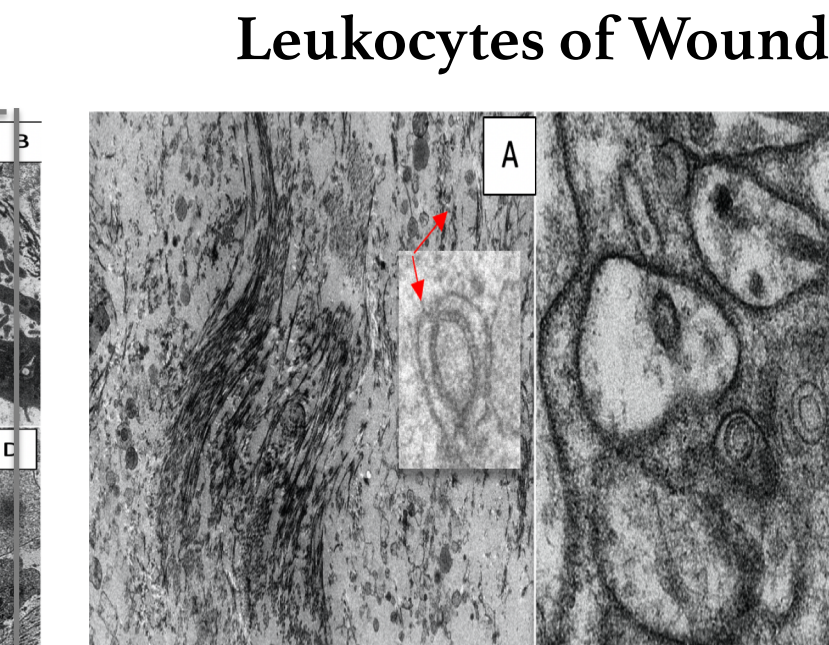


Figure 21. Unknown cell types observed in wound under TEM.

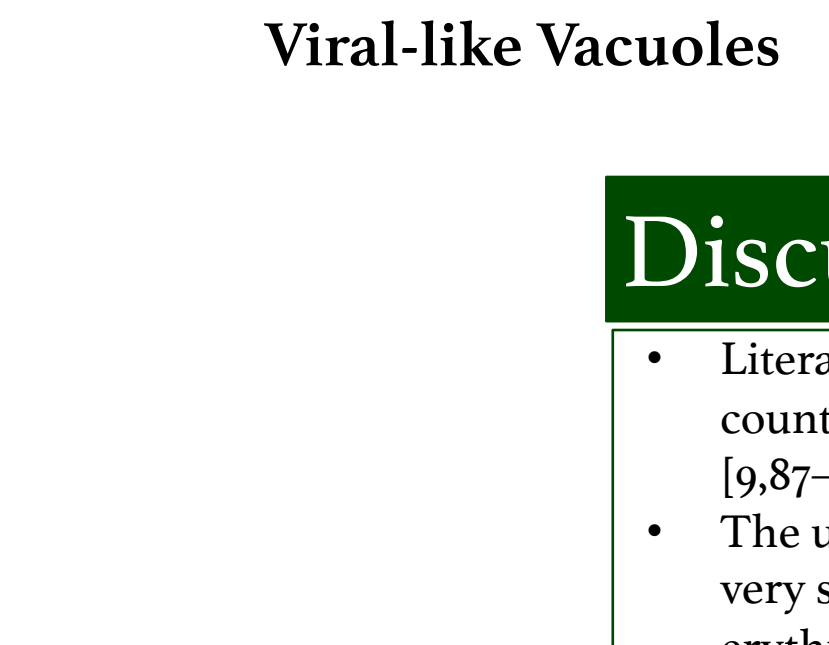


Figure 21. Unknown cell types observed in wound under TEM.

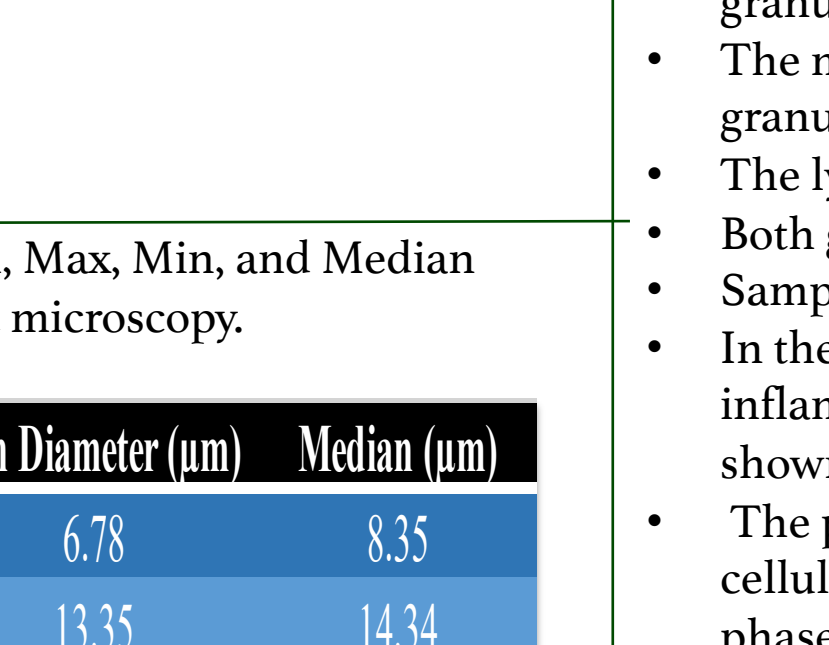


Figure 21. Unknown cell types observed in wound under TEM.



Figure 21. Unknown cell types observed in wound under TEM.

Discussion

- Literature regarding the hematology of elasmobranchs is limited, with many concluding peripheral blood counts as inaccurate; as manual counts are the only means of quantifying the hematology of elasmobranchs [9,87-89].
- The ultrastructure of the erythrocyte in SEM showed the presence of pores around the membrane with very similar sizes and distributions. Erythroblasts in SEM had the same porous membrane as the erythrocyte, but at a much higher concentration.
- Granulocytes of the bull shark consisted of the course eosinophil granulocyte (CEG), course eosinophilic granulocyte-2 (CEG2), fine eosinophilic granulocyte, and neutrophil.
- The monocyte was shown to be agranular and is significantly smaller than the erythrocyte and granulocytes.
- The lymphocyte is found in the highest concentration and variability out of all cell types.
- Both granulated thrombocytes and thrombocytes were found in the blood.
- Sample N395491 was the shark that presented the wound to the SRC team.
- In the wound biopsy regions of pink tissue and blue tissue were collected. Regions of pink were areas of inflammation and likely were farther along in the wound healing process. While regions of blue were shown to be regions of high inflammatory response.
- The pink section biopsy showed significantly higher levels of re-epithelization as present by the increase in cellular organization displayed in figure 28. This organization is believed to be a part of the cell proliferation phase of wound healing [61].
- This can be further viewed by the formation of 'progenitor' type placoid denticle forming cell structures as seen in figure 25.
- The blue portion of the wound contains a larger influx of leukocytes, apoptotic erythrocytes, fibroblasts, and cellular debris, as seen in figure 29.
- The widespread cellular debris has led to speculation on many cell types present in electron microscopy imaging of this wound healing process, as possible dendritic, mast, and macrophage-like cell types were observed sharing similar morphologies to these cell types found in varying other organisms [36,56,57,90-92]. This wound is still largely involved in the inflammatory response of wound healing, as further illustrated by presence of plasma-like cells as seen in figure 22.
- From limited past literature it can be inferred that this wound is between one and three weeks old, with the initial lesion still sealing and likely caused by a fishing hook.

Acknowledgments

This study would not have been possible without the tireless efforts of Dr. Liza Merly, Dr. Patricia Blackwelder, Dr. Donald Olson, and the UM Shark Research and Conservation Program.

References

1. Marra et al. 2019 2. Smith et al. 2019 3. Chin et al. 2015 4. McGregor et al. 2019 5. McKinney et al. 1992 6. Obenauf et al. 1985 7. Moore et al. 1993 8. Hibbit et al. 2017 9. Smith et al. 2014 10. Mumford et al. 2007 11. Maceida-veiga et al. 2015 12. Cheng et al. 2016 13. Gallagher et al. 2014 14. Arnold et al. 2005 15. Clauss et al. 2008 16. Parish et al. 1986 17. Leur et al. 2004 18. Gonzalez et al. 2016 19. Ellis et al. 1977 20. Ohta et al. 2004 21. Bassity et al. 2012 22. Fischer et al. 2013 23. Kordon et al. 2016 24. Fujii et al. 1999